Plasminogen Kringle 5–Engineered Glioma Cells Block Migration of Tumor-Associated Macrophages and Suppress Tumor Vascularization and Progression

Sabrina R. Perri,[1,2] Josephine Nalbantoglu,[3] Borhane Annabi,[6] Zafiro Koty,[4] Laurence Lejeune,[2] Moïra François,[2] Marcos R. Di Falco,[5] Richard Béliveau,[7] and Jacques Galipeau[1,2,8]

[1]Division of Experimental Medicine, [2]Lady Davis Institute for Medical Research; [3]Department of Neurology and Neuroscience, [4]Montreal Neurological Institute, McGill University; [5]McGill University and Genome Quebec Innovation Centre; [6]Department of Biochemistry, [7]Laboratoire de Médicine Moléculaire, Centre de Cancérologie Charles-Bruneau, Hôpital Sainte-Justine, Université de Québec à Montréal; and [8]Division of Hematology/Oncology, Department of Medicine, Jewish General Hospital, Montreal, Quebec, Canada

Abstract

Angiostatin, a well-characterized angiostatic agent, is a proteolytic cleavage product of human plasminogen encompassing the first four kringle structures. The fifth kringle domain (K5) of human plasminogen is distinct from angiostatin and has been shown, on its own, to act as a potent endothelial cell inhibitor. We propose that tumor-targeted K5 cDNA expression may act as an effective therapeutic intervention as part of a cancer gene therapy strategy. In this study, we provide evidence that eukaryotically expressed His-tagged human K5 cDNA (hK5His) is exported extracellularly and maintains predicted disulfide bridging conformation in solution. Functionally, hK5His protein produced by retrovirally engineered human U87MG glioma cells suppresses *in vitro* migration of both human umbilical vein endothelial cells and human macrophages. Subcutaneous implantation of Matrigel-embedded hK5His-producing glioma cells in nonobese diabetic/severe combined immunodeficient mice reveals that hK5His induces a marked reduction in blood vessel formation and significantly suppresses the recruitment of tumor-infiltrating $CD45^{+}Mac3^{+}Gr1^{-}$ macrophages. Therapeutically, we show in a nude mouse orthotopic brain cancer model that tumor-targeted K5 expression is capable of effectively suppressing glioma growth and promotes significant long-term survival (>120 days) of test animals. These data suggest that plasminogen K5 acts as a novel two-pronged anticancer agent, mediating its inhibitory effect via its action on host-derived endothelial cells and tumor-associated macrophages, resulting in a potent, clinically relevant antitumor effect. (Cancer Res 2005; 65(18): 8359-65)

Introduction

Glioblastomas are very aggressive solid tumors characterized by hypervascularization and extensive tumor cell invasion into normal brain parenchyma (1). Current therapeutic modalities primarily target rapidly dividing malignant cells and include combinations of surgery, radiotherapy, and chemotherapy (1, 2). However, these therapies remain ineffective with >90% of patients experiencing local recurrence and a 5-year survival rate of only 9% (3).

The urgent need for the development of potent antiglioma therapeutics as well as the importance of angiogenesis in glioma growth (4, 5) has fueled the identification and characterization of numerous antiangiogenic agents, aimed at interrupting new vessel formation and ultimately arresting tumor growth. The use of antiangiogenic agents as therapeutics is an appealing approach targeting nonmalignant endothelial cells that form the tumor vasculature and indirectly affects tumor cells thus minimizing the risk of toxicity. In addition, the problem of drug resistance associated with conventional chemotherapy agents is avoided because normal endothelial cells are genetically stable unlike tumor cells (6). Moreover, the blood-brain barrier is another obstacle often encountered with therapies targeting malignant cells within the brain and may be exploited with antiangiogenic strategies by maintaining the angiogenic inhibitor within the brain vasculature for a prolonged period. Although angiogenesis inhibition offers several advantages over traditional therapeutic approaches, it is expected to induce a cytostatic effect resulting in tumor stabilization not eradication. Furthermore, single-agent antiangiogenic therapy may lead to a compensatory increase in the production of other angiogenic factors, which may then sustain angiogenesis (1). Despite these limitations, it is now well recognized that angiostatic agents either singly or in combination with other treatment modalities could offer superior therapeutic benefits than currently attainable (7–13), converting the tumor into a controlled, quiescent chronic disease. Direct delivery of purified recombinant antiangiogenic proteins however necessitates large quantities and repeated administration of the therapeutic gene product for a prolonged period of time (14, 15). To circumvent the pitfalls associated with conventional treatments, we have developed a potent antiangiogenic gene therapy strategy for brain cancer. Moreover, because malignant gliomas localize within the central nervous system and do not form distant metastases (16), they represent an attractive target for local gene therapy, which provides high and sustained local production of the desired therapeutic agent and offers a viable alternative to existing therapeutic interventions.

Several inhibitors of angiogenesis exist endogenously as proteolytic cleavage products of larger precursor molecules. Angiostatin, a well-characterized antiangiogenic agent discovered by O'Reilly et al. in Folkman's laboratory, was initially identified as an endothelial cell growth inhibitor present in urine and plasma of animals harboring solid tumors (17, 18), is an internal cryptic fragment of human plasminogen encompassing the first four kringle (K1-4) domains (Fig. 1*A*). The K5 domain of plasminogen has been

Note: Supplementary data for this article are available at Cancer Research Online (http://cancerres.aacrjournals.org/).

Requests for reprints: Jacques Galipeau, Lady Davis Institute for Medical Research, 3755 Cote-Ste-Catherine Road, Montreal, Quebec, Canada H3T 1E2. Phone: 514-340-8214; Fax: 514-340-8281; E-mail: j.galipea@lab.jgh.mcgill.ca.

doi:10.1158/0008-5472.CAN-05-0508

expressed as a recombinant protein in bacteria and been found to be more potent than K1-4 or any of the plasminogen kringles expressed individually in inhibiting growth factor stimulated proliferation of endothelial cells *in vitro* (19, 20). It has also been shown that kringle domains 1-5 (K1-5) act as more potent endothelial cell inhibitors *in vitro* and are more effective in suppressing fibrosarcoma tumor growth *in vivo* compared with K1-4 alone (21). We propose that the K5 domain could serve as a potent angiostatic agent on its own and that it may act as a useful therapeutic transgene within a cancer gene therapy strategy. To test this hypothesis, we have developed a human K5-expressing retroviral vector and tested its efficacy *in vivo* using an orthotopic brain cancer model.

Materials and Methods

Cell culture reagents. 293GPG pantropic retrovirus-packaging cell line (22) was a gift from Dr. Richard C. Mulligan (Children's Hospital, Boston, MA). Human glioma U87MG cell line (23) was a gift from Dr. Stéphane Richard (Lady Davis Institute, Montreal, Quebec, Canada). Freshly isolated primary human umbilical endothelial cells (HUVEC) were generously provided by Dr. Mark Blostein (Lady Davis Institute) and maintained in endothelial-basal media (EBM-2; Cambrex, Walkersville, MD) supplemented with EBM-2 SingleQuots. Fresh human peripheral blood mononuclear cells were obtained from normal volunteers and maintained in DMEM-F12 (Wisent Technologies, St-Bruno, QC, Canada) supplemented with 2% human serum and 500 units/mL granulocyte/macrophage colony stimulating factor (GM-CSF; Immunex, Thousand Oaks, CA).

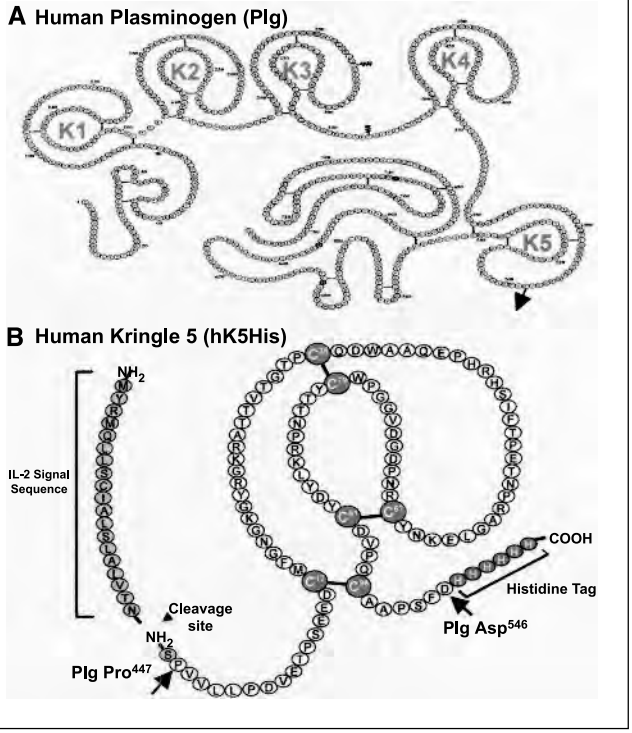

Figure 1. Schematic illustration of human plasminogen (*Plg*) and its kringle domains. *A,* plasminogen is composed of 791 amino acids with a single N-linked glycosylation at Asn^{289} and a single O-linked glycosylation at Thr^{346}. Angiostatin, a well-known inhibitor of angiogenesis, encompasses the first three to four kringle structures of plasminogen. This is a modified schematic courtesy of Dr. M.R. Llinás et al., Carnegie Mellon University, Pittsburgh, PA (http://www.chem.cmu.edu/groups/Llinas/res/structure/hpk.html). *B,* hK5 consists of the last cryptic fragment of plasminogen (Cys^{462}-Cys^{541}) and is composed of 80-amino-acid residues with three distinct disulfide bonds.

Soluble human kringle 5-hisTag expression vector, protein purification, and detection. pBLAST-hK5 cDNA (InvivoGen, San Diego, CA) encodes for hK5 and contains a 5′ interleukin-2 signal peptide (IL-2sp) coding sequence. A 3′ 6-histidine tag was PCR cloned to generate IL-2sp/hK5/HisTag (hereafter hK5His). Conditioned medium was collected from hK5His stably transfected human kidney 293 T cells, concentrated using a Centricon Plus-20 column (Millipore, Billerica, MA) and purified using a Ni-NTA-based resin affinity chromatography purification system (Novagen, San Diego, CA). Immunoblot analysis was done on eluted fractions using a polyclonal anti-His antibody (Santa Cruz Biotechnology, Santa Cruz, CA).

Proteomic analysis of purified soluble hK5His. Lyophilized hK5His samples were resuspended in water/5% acetonitrile/0.1% trifluoroacetic acid (TFA), desalted using reverse-phase C18 ZipTips (Millipore), eluted with water/70% acetonitrile/0.1% TFA. The eluate was spotted onto a matrix-assisted laser desorption ionization (MALDI) sample plate and analyzed using a MALDI time-of-flight (TOF) Voyager-DE (Applied Biosystems, Foster City, CA). The eluted fraction was also spotted onto polybrene-coated TFA filter discs for Edman degradation-based NH_2-terminal sequence analysis using a Procise 492 automated microsequencer (Applied Biosystems). One eluate aliquot was treated with 10 mmol/L DTT for 1 hour, diluted with 80 μL of 50 mmol/L Ambic containing 100 ng of Trypsin gold (Promega, Madison, WI), and digested overnight. For dual-enzyme digest, the eluted fraction was first digested overnight with immobilized trypsin (Pierce, Rockford, IL) followed by an overnight digestion with 100 ng of Endoproteinase-Asp-N (Roche Diagnostics, Laval, Quebec, Canada). Digested solutions were ziptipped and eluted onto a MALDI sample plate. Peptide fragment analysis was done with an Ultima MALDI-Quadrupole TOF mass spectrometer (Waters Limitée, Dorval, Quebec, Canada). Spectra analysis and peptide identity assignment was done using Biolynx, a software tool of Masslynx v4.0 (Waters).

VSV-G-pseudotyped retroviral vector design, synthesis, and titer assessment. The bicistronic murine retrovector pIRES-EGFP was previously generated in our laboratory (24) and contains an enhanced green fluoescent protein (EGFP). The hK5His cDNA was ligated into pIRES-EGFP to generate phK5His-IRES-EGFP. VSV-G-pseudotyped retroparticles encoding hK5His-IRES-EGFP were generated by tetracycline withdrawal as previously published (24, 25). Engineered retroparticles were devoid of replication-competent retrovirus as determined by GFP marker rescue assay using conditioned medium from target cells. The titer of the control GFP and hK5His 293GPG single clone population was assessed as previously described (25).

Transduction of human U87MG glioma cells. Glioma cells were transduced with hK5His-expressing retroviral particles as previously described (24). Stably transduced glioma cells were culture expanded and sorted to obtain both polyclonal and single clone populations based on GFP expression using a Becton Dickinson FACSTAR sorter.

Western blot analysis. Conditioned medium was collected from confluent control GFP and hK5His-transduced U87 glioma cells, as well as stably transfected hK5His 293 T cells (positive control), concentrated, and detected by anti-His immunoblot analysis as previously mentioned.

Migration assays. HUVEC (1×10^4) or human macrophages (5×10^4) were plated onto 0.15% gelatin/PBS-coated 8-μm pore chemotaxis membranes (Corning, Acton, MA) within Boyden chamber inserts. Migration assays were done as previously described (26). HUVEC and macrophages were exposed to conditioned medium from control GFP and hK5His transduced U87 glioma cells for 4 and 24 hours, respectively, under growth factor–stimulated conditions (EBM-2 SingleQuots) and serum stimulation, respectively. Each sample was tested in triplicate and the average number of migrating cells per field was assessed by counting three random high-power fields per filter.

***In vivo* Matrigel assay and analysis of cellular infiltrate by cytometry.** Culture-expanded U87-GFP and U87-hK5His-GFP cells were aliquoted to create 50-μL cell suspensions containing 2×10^4 cells, mixed with 500 μL Matrigel (BD Biosciences, San Jose, CA) at 4°C, and implanted s.c. in the right lateral flank of 6-week-old nonobese diabetic/severe

combined immunodeficient (NOD-SCID) mice (Charles River, Laprairie, Quebec, Canada). Four weeks after implantation, mice were sacrificed and implants excised and processed as previously described (27). To determine the explant cellular infiltrate, cell suspensions were stained with the following antibodies: purified rat anti-mouse CD16/CD32 (mouse Fc block) followed by APC-conjugated rat anti-mouse CD45, PE-conjugated rat anti-mouse Mac-3, biotin-conjugated rat anti-mouse Ly-6G (Gr-1), and their corresponding isotypic controls. Biotinylated antibodies were revealed using PE-Cy7-streptavidin (BD PharMingen, San Diego, CA). Cells were fixed with 1% paraformaldehyde and events were acquired using a FACSCalibur flow cytometer (Beckman Coulter, Fullerton, CA) and analyzed using the CellQuest software (BD PharMingen).

Matrigel explant histochemistry. Explants were fixed in formalin, embedded in paraffin, and 4-μm sections were prepared to generate representative sections of the border and central regions of the explants. Sections were treated with xylene, rehydrated, and antigen retrieval was done using two microwave boils in a 10 mmol/L sodium citrate buffer (pH 6.0) solution. Endogenous biotin activity was blocked using a kit (Zymed Laboratories, Markham, Ontario, Canada), sections were subsequently blocked with 2.5% bovine serum albumin in PBS and incubated with a rabbit polyclonal raised against murine von Willebrand factor (vWF; Neomarkers, Fremont, CA dilution 1:100) overnight. After three washes, the sections were incubated with biotinylated goat anti-rabbit IgG antibody (BD PharMingen, dilution 1:200) for 2 hours, washed, and incubated with streptavidin-peroxidase (Vector Labs, Burlingame, CA) for 1 hour before the addition of 3,3′-diaminobenzidine chromogenic substrate (Vector Labs). Meyer's hematoxylin was used for counterstaining. The blood vessel surface area of all vWF-positive vessels was calculated using a Leica light microscope ocular micrometer (Leica Microsystems, Inc., Richmond Hill, Ontario, Canada) at 400× magnification. Two observers counted three random sections per explant in each experimental group. The blood vessel surface area to total section surface area was calculated and expressed as a percentage.

Stereotactic intracerebral surgery. CD1 *nu/nu* female 6-week-old athymic nude mice (Charles River) were anesthetized using a ketamine/xylezine/saline/acepromazine cocktail (100 mg/mL, 20 mg/mL, 0.9%, 10 mg/mL, respectively) dosed at 100 μL/100 g by i.p. injection. Mice were secured in stereotactic apparatus (Kopf Instruments, Tujunga, CA) and incisor bar set to −1.5. Midline incision made on scalp to expose Bregma and Lambda. Coordinates from Bregma were AP, +0.5; LM, −2.0; and DV, −4.4. A burr hole was made and a Hamilton syringe (10-μL 26-gauge needle, Hamilton Co., Reno, NV) was gently lowered. Cell suspension (1×10^5 in 3 μL of HBSS) was injected at a rate of 0.25 μL per 3 minutes for 36 minutes.

Brain tissue analysis. After euthanasia, brains were processed for H&E staining as previously described (28). Digital images were retrieved using an Olympus microscope (Olympus America, Melville, NY). Tumor volumes were calculated using the formula, length × width^2 × 0.4.

Results

Matrix-assisted laser desorption ionization-quadrupole time-of-flight mass spectrometry analysis of expressed soluble hK5His peptide confirms predicted disulfide bridging conformation. The 381-bp human plasminogen K5 domain cDNA, corresponding to amino acid residues 447 to 546 of plasminogen, includes a 20-amino-acid IL-2 signal sequence and a His-tag at the COOH terminus (Fig. 1*B*) and encodes for the hK5His protein with a kringle structure as predicted by previously published nuclear magnetic resonance (NMR) structure study (29). Affinity chromatography was done on precleared conditioned medium from stably transfected hK5His-expressing 293T cells. Anti-His immunoblot, following SDS-PAGE separation (Fig. 2*A, top*), shows a major band of 15 kDa (Fig. 2*A, bottom*). NH_2-terminal amino acid sequencing indicated proper cleavage of the IL-2 signal sequence directly upstream of Ser^{20} and analysis by MALDI-Q TOF mass spectrometry revealed a major peak at 12,108 Da consistent with the predicted molecular weight of hK5His (Fig. 2*B*). To fully characterize cystinyl bridge structure and confirm kringle domain tertiary structure, an orthogonal digestion was carried out either with agarose-immobilized trypsin alone (Fig. 2*C*) or with trypsin followed by incubation with Asp-N endopeptidase (Fig. 2*D*) under reducing and nonreducing conditions. Peptide mapping of non-reduced single and dual protease hK5His digests by MALDI-Q TOF mass spectrometry confirmed the presence of disulfide bridges among Cys^{17}-Cys^{96}, Cys^{38}-Cys^{79}, and Cys^{67}-Cys^{91} (by deduction). These findings show that plasminogen hK5His domain spontaneously adopts a tertiary structure consistent with native conformation as displayed within plasminogen when expressed by genetically engineered eukaryotic cells.

hK5His protein secreted by retrovirally gene-modified human glioma cells inhibits *in vitro* endothelial cell migration. The hK5His cDNA was cloned into our previously published (24) bicistronic retroviral vector (Fig. 3*A*). The hK5His retrovector plasmid was stably transfected into 293GPG retroviral packaging

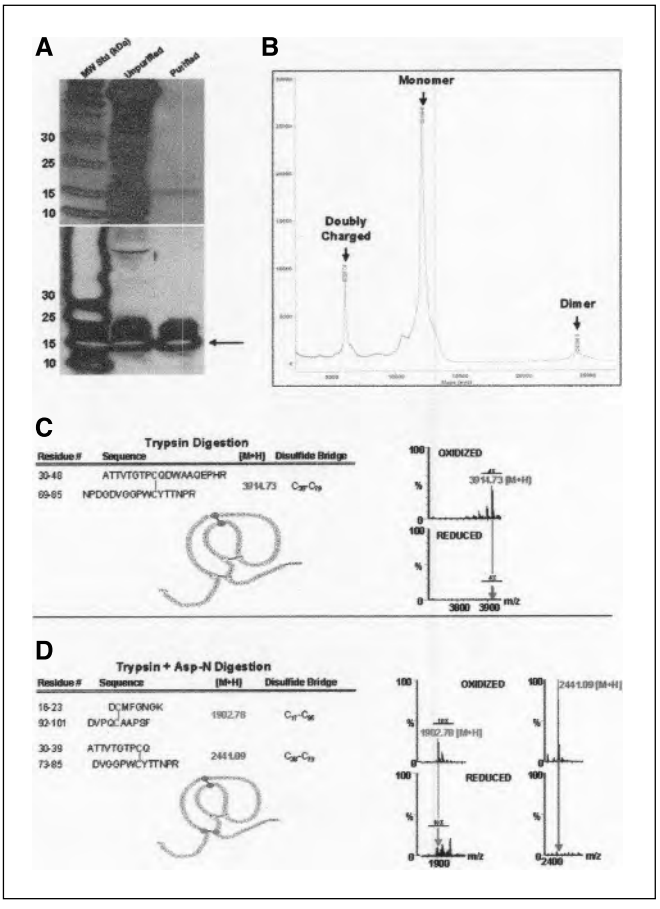

Figure 2. Proteomic analysis of purified soluble hK5His. *A,* silver stain done on pooled eluted fractions detects purified protein at the expected molecular weight of 15 kDa (*top*). Anti-His immunoblot analysis demonstrates the presence of soluble hK5His peptide in pooled eluted fractions (*bottom*). *B,* analysis of the purified hK5His peptide by MALDI-Q TOF mass spectrometry revealed a major peak at 12,108 Da consistent with the theoretical molecular weight of monomeric K5 at 12,109.6 Da. The doubly charged form and dimer are detectable at 6,059 and 24,195 Da, respectively. *C,* expected peptide fragment of interest generated for hK5His protein digested with trypsin alone under oxidizing conditions (*left*). *C,* MALDI-Q TOF mass spectra confirming Cys$^{38:79}$ disulfide bond within hK5His (*right*). *D,* expected peptide fragment of interest generated for hK5His protein digested with trypsin followed by Asp-N endopeptidase treatment under oxidizing conditions (*left*). Spectra confirming Cys$^{17:96}$ and Cys$^{38:79}$ disulfide bonds (*right*).

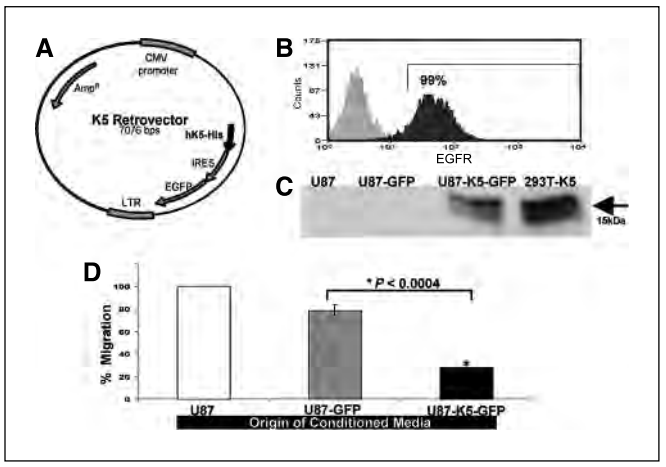

Figure 3. Development and characterization of hK5His-GFP gene-modified cells. *A,* schematic illustration of the human hK5His-IRES-EGFP retroviral plasmid construct. The retrovector pIRES-EGFP construct served as the control plasmid. *B,* flow cytometry analysis of untransduced (*gray*) and hK5His-transduced (*black*) human U87 glioma cells. *C,* anti-His immunoblot analysis reveals functional secretion of hK5His migrating as a doublet at ~15 kDa from retrovirally gene-modified U87 glioma cells and stably transfected 293T cells (positive control). *D,* conditioned medium from hK5His-transduced glioma cells inhibits HUVEC migration up to 75 ± 3%. *Bars,* SE. Statistical analysis was done using Student's *t* test.

cells and retrovirus producer cells were selected as described in Materials and Methods. Tetracycline withdrawal from the culture medium led to the production of VSV-G-typed hK5His-GFP retroviral particles that were subsequently concentrated 100-fold by ultracentrifugation and a viral titer of $\sim 2.5 \times 10^6$ infectious particles/mL was obtained (data not shown). Concentrated VSV-G-typed hK5His-GFP retroviral particles were used to transduce human glioma cells. The U87MG human glioblastoma cell line was selected for this study because it overexpresses vascular endothelial growth factor (VEGF)–producing tumors *in vivo* that are characterized by increased vascularity, lack of necrosis, and absence of peripheral invasion in early tumor development (1). Following retroviral transduction, single U87MG clones were selected and assessed for GFP expression by flow cytometry. The U87 single clone used for the study was sorted based on GFP expression and was 99% GFP positive (Fig. 3*B*). To ensure hK5His transgene expression and proper secretion, anti-His immunoblot analysis was done on conditioned supernatant collected from hK5His transduced human U87 glioma cells and detects a major 15-kDa protein consistent with the predicted molecular weight of soluble hK5His (Fig. 3*C*). Using a semiquantitative Western blot titration curve, it was estimated that hK5His-GFP-expressing U87 cells secrete 0.5 pmol/L (or 7.5 ng) of soluble hK5His per 10^6 cells per 24 hours (data not shown). To test the functionality of secreted hK5His from hK5His-GFP-expressing U87 cells, a HUVEC migration assay was done as it has been previously shown that recombinant K5 protein is capable of inhibiting the migration of bovine capillary endothelial cells (30). Soluble hK5His present in the conditioned medium of hK5His-GFP-expressing U87 cells was capable of inhibiting growth factor–induced migration of HUVEC up to 75 ± 3% ($P < 0.0004$) compared with conditioned medium from GFP-expressing U87 cells (Fig. 3*D*). This confirms the *in vitro* functionality of hK5His secreted by hK5His-GFP-expressing U87 cells.

hK5His blocks glioma-associated angiogenesis and possesses novel antimacrophage properties. To further characterize the mechanism of action of soluble hK5His *in vivo*, we investigated whether hK5His could interfere with the tumor microenvironment. More specifically, we assessed whether soluble hK5His could affect the recruitment of host-derived tumor-infiltrating endothelial as well as inflammatory cells implicated in tumor angiogenesis. To test this hypothesis, 2×10^4 U87-GFP ($n = 10$) or U87-hK5His-GFP ($n = 10$) cells were Matrigel embedded and implanted s.c. in NOD-SCID mice. To verify if tumor-secreted hK5His induced an antiangiogenic effect *in vivo*, explants ($n = 4$) in each experimental group were retrieved 4 weeks after implantation (Fig. 4*A*) and stained with vWF antibody (Fig. 4*B*). The section surface area occupied by vWF-positive blood vessels to total section surface

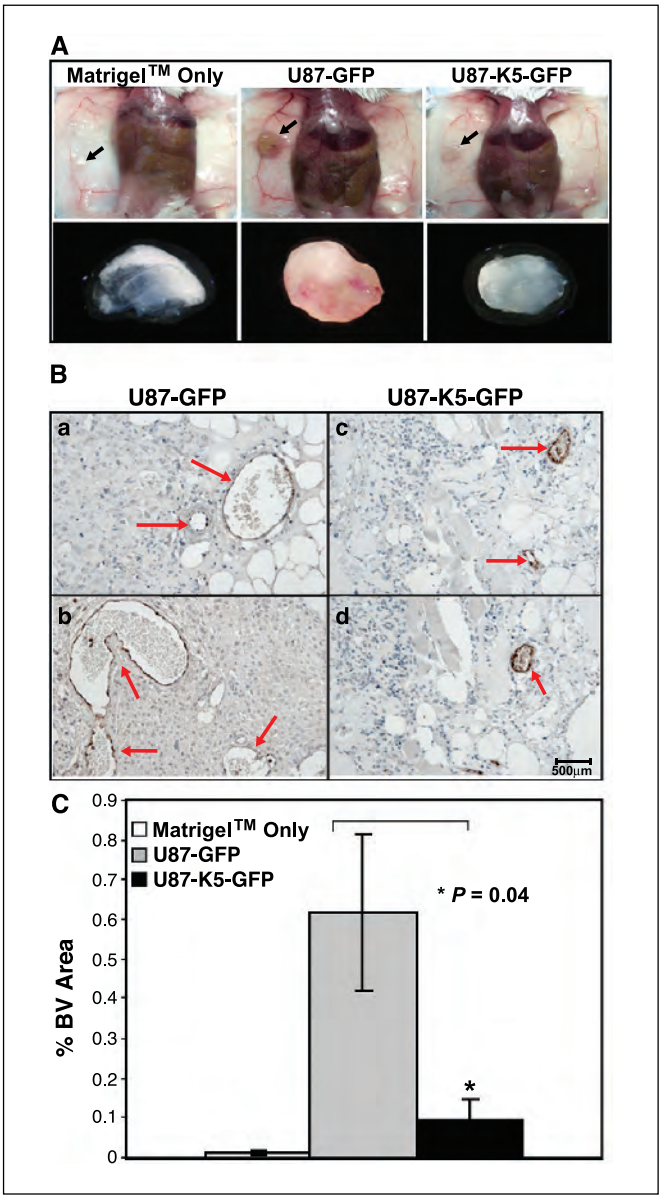

Figure 4. hK5His acts as a potent antiangiogenic agent. *A,* implant (*arrow*) retrieval 4 weeks after implantation of 2×10^4 Matrigel-embedded U87-GFP or U87-hK5His-GFP cells (representative images are shown at the same magnification). *B,* representative images of vWF-positive immunostained blood vessels (*red arrows*) from two different U87-GFP-containing (*a* and *b*) and U87-hK5His-GFP-containing (*c* and *d*) implants; magnification, 200×. *C,* vWF-positive blood vessel surface area to total section surface area ratio is plotted as a percentage. *Bars,* SE (SE for Matrigel-only group was based on three random section counts from one animal because remaining implants resorbed completely). Statistical analysis was done using Student's *t* test.

area ratio was calculated and expressed as a percentage (Fig. 4*C*). Our results show that soluble hK5His domain is capable of exerting a potent antiangiogenic effect ($P = 0.04$) *in vivo* when secreted by retrovirally engineered glioma cells. The remaining explants ($n = 6$) in each experimental group were dissolved in a collagenase solution and single-cell suspensions were generated and counted. (Fig. 5*A, left*). The hK5His-GFP explants contained about two thirds less cells than the control GFP explants ($P = 0.01$). The cellular infiltrate in the explants was analyzed for GFP expression as well as for cell surface marker expression to distinguish the various cell types present within the explants (Fig. 5*A, right*). The GFP-positive cell fraction representing glioma cells is significantly reduced in the hK5His-GFP explants compared with the control GFP explants ($P = 0.03$). It is important to note that the difference in absolute tumor cell number is not due to differences in the proliferation rates of the control GFP and hK5His-GFP glioma cells because both possess equivalent proliferation rates *in vitro* (Supplementary Fig. 1). Although immunocompromised NOD-SCID mice possess functional macrophages and granulocytes, they lack functional T and B lymphocytes. Flow cytometry analysis after three-color staining indicated that a substantial part of the cellular infiltrate consisted of CD45-positive hematopoietic cells (Fig. 5*B, left*). More specifically, there was a reduced absolute number of recruited $CD45^+Mac^+Gr1^+$ ($P = 0.04$) cells, which represents the monocyte/macrophage fraction and $CD45^+Mac3^+Gr1^-$ ($P = 0.03$) cells, which represents the macrophages present in the U87-hK5His-GFP-containing explants compared with the control U87-GFP-containing explants (Fig. 5*B*). There was no significant difference in the number of $CD45^+Mac3^-Gr1^+$ ($P = 0.43$) cells representing the infiltrated granulocytes present in the explants.

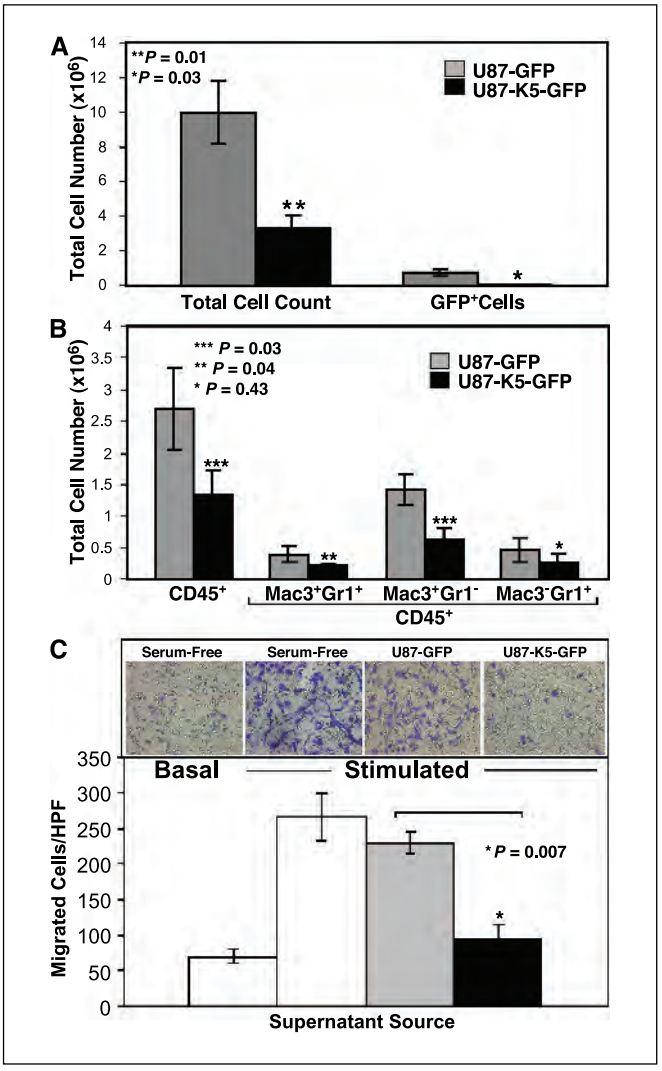

Figure 5. hK5His possesses novel antimacrophage property and decreases migration potential of human macrophages. *A,* absolute total cell count performed after collagenase digestion of the explants (*left*). Absolute number of GFP positive cells was enumerated using flow cytometry and represents the GFP-marked glioma cells (*right*). *Bars,* SE. *B,* absolute number of infiltrated $CD45^+$ hematopoietic cells, $CD45^+Mac3^+Gr1^+$ monocytes/macrophages, $CD45^+Mac3^+Gr1^-$ macrophages and $CD45^+Mac3^-Gr1^+$ granulocytes in the explants. *Bars,* SE. Statistical analysis was done using Student's *t* test. *C,* macrophages were exposed to various conditioned medium for 24 hours under serum stimulation. Basal invasion represents migrating macrophages under serum-free conditions. *Bars,* SE. *Insets,* representative stains of migrated cells from each experimental group; magnification, 200×. Statistical analysis was done using Student's *t* test.

To confirm our *in vivo* observations, we tested whether hK5His could inhibit macrophage migration *in vitro*. A migration assay was done using human monocytes isolated from peripheral blood mononuclear cells that were stimulated with GM-CSF to differentiate into $CD206^+$ macrophages (data not shown). The ability of macrophages to migrate through a gelatin matrix was assessed under serum-stimulated conditions, where macrophages were directly exposed to conditioned medium collected from GFP-expressing glioma cells and hK5His-GFP-expressing glioma cells. The results indicate that soluble hK5His decreases the migration potential of human macrophages by ~60% compared with the GFP control ($P = 0.007$, Fig. 5*C*).

Glioma-targeted hK5His expression suppresses tumor growth and prolongs survival in an experimental orthotopic brain cancer model. To test the efficacy of retrovirally engineered glioma cells secreting hK5His in a clinically relevant proof-of-principle experiment, 10^5 U87-GFP ($n = 5$) and U87-hK5His-GFP cells derived from either a single clone ($n = 5$) and an independently generated polyclonal population ($n = 5$) were implanted intracerebrally in athymic *nu/nu* (nude) mice. Mice were sacrificed 32 days after implantation and brains were removed and processed for H&E staining (Fig. 6*A*). Tumor volumes from each experimental group were estimated from H&E-stained cryostat sections and calculated as described in Materials and Methods. Consistent with our previous study (28), brain tumors in the GFP control group had extensive growth. In contrast, the U87-hK5His-GFP-implanted mice possessed significantly reduced mean tumor volumes (0.35 ± 0.18 mm^3 for the single clone population and 0.07 ± 0.03 mm^3 for the polyclonal population) compared with the control U87-GFP-implanted (12.23 ± 6.07 mm^3) mice ($P = 0.04$; Fig. 6*B*).

We did a long-term *in vivo* study, where we evaluated the survival of the therapeutic cohort implanted with U87-hK5His-GFP cells ($n = 15$) and the control U87-GFP-implanted ($n = 10$) mice. Although all control mice succumbed to excessive tumor burden by ~8 weeks, the U87-hK5His-GFP-implanted mice possessed a clear survival advantage with 53% of the mice surviving over 120 days ($P < 0.0001$; Fig. 6*C*).

Discussion

This present study shows that eukaryotically expressed secreted hK5His protein preserves the prototypical native kringle disulfide bridging conformation deemed essential for the angiostatic activity of plasminogen-derived peptide domains. Indeed, our cysteine

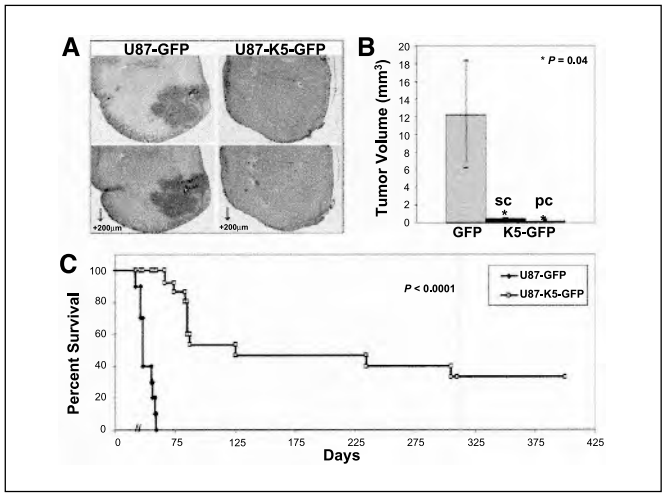

Figure 6. Suppression of intracerebral U87MG glioma growth by soluble hK5His. *A,* H&E-stained brain tissue sections from control U87-GFP implanted mice (n = 5) and U87-hK5His-GFP implanted mice (n = 5) 32 days after implantation. Representative stains are shown at the same magnification, 40×. *B,* tumor volumes were estimated from postmortem H&E-stained brain sections obtained from mice implanted with U87-GFP, U87-hK5His-GFP single clone (*sc*), and U87-hK5His-GFP polyclonal (*pc*) cells. The experiment was done twice with similar results. *Bars,* SE. Student's t test. *C,* Kaplan-Meier long-term survival curve of mice implanted with control U87-GFP (n = 10) and U87-hK5His-GFP (n = 15) cells. Log-rank statistical test.

bridging pattern data confirms the results of the only other study that characterizes the structure of recombinant K5 domain using NMR technology (29). We have shown that VSV-G-pseudotyped retroviral vectors engineered to express human plasminogen hK5His domain can efficiently gene modify human U87 glioma cells *ex vivo.* We also show that hK5His-engineered U87 cells can secrete biologically functional soluble hK5His protein capable of inhibiting growth factor–stimulated endothelial cell migration *in vitro*.

Moreover, our *in vivo* data in immunodeficient NOD-SCID mice suggests that hK5His secreted by Matrigel-embedded U87 engineered cells acts as a potent antiangiogenic agent by significantly decreasing blood vessel formation as well as a novel antimacrophage agent by significantly preventing the recruitment of host-derived tumor-associated $CD45^{+}Mac3^{+}Gr1^{+/-}$ monocytes/macrophages within the local tumor microenvironment. The involvement of tumor-associated macrophages in angiogenesis and tumor progression is a well-established concept (31–33). Activated macrophages produce tumor necrosis factor-α and IL-1, inducing the production of VEGF and IL-8 in glioma cells, which further attracts and activates macrophages (34). Macrophage infiltration has been closely correlated with neovascularization and observed more frequently in grade 4 glioblastomas than in grade 2 or 3 gliomas (34).

It may be speculated that the potent antiangiogenic properties of soluble K5 mediating a reduction in tumor-associated endothelial cells, as evidenced by the lower surface area occupied by blood vessels in the U87-hK5His-GFP-containing explants, is partially responsible for the decreased infiltration of host-derived macrophages within the tumor area. We also show that soluble hK5His independently reduces macrophage migration *in vitro*, suggesting that the K5 domain can impart a direct inhibitory effect on macrophage motility. To date, the K5 peptide has been consistently characterized as an endothelial cell–specific inhibitor (19, 30) and Gonzalez-Gronow et al. (35) suggest that K5 mediates its effects by binding to the human voltage-dependent anion channel, which is a receptor present on human endothelial cells. Unlike K5, the mechanism of action of angiostatin has been studied more extensively and its endothelial cell binding sites include the cell surface–associated ATP synthase receptor (36), angiomotin (37), and integrin $\alpha_v\beta_3$ (38). Although angiostatin mediates its inhibitory action primarily on endothelial cells, it has been reported by Moulton et al. (39) that it reduces plaque angiogenesis and atherosclerosis by reducing plaque-associated macrophages. However, Moulton et al. suggest that angiostatin, at doses that reduce endothelial cell sprouting, does not directly inhibit monocytes because it does not inhibit VEGF-induced monocyte migration *in vitro*. Thus, our findings provide novel mechanistic insight and suggest that soluble hK5His protein inhibits two unique cell types most critical for tumor angiogenesis, mediating a dual role as an antiangiogenic agent via its antiendothelial cell properties as well as an antitumor agent by reducing the infiltration of host-derived macrophages within the tumor microenvironment.

We used a clinically relevant orthotopic implantation approach to test whether soluble hK5His could suppress glioma progression after implantation of hK5His-GFP-expressing U87 cells in athymic *nu/nu* mice. Stereotactic implantation procedures are particularly suitable for glioma gene therapy approaches allowing for constant long-lasting transgene expression within the local tumor microenvironment and minimize the risk of toxicity as is often encountered with systemic therapies. Our data successfully shows that soluble hK5His significantly decreases tumor growth by ~97% compared with controls. In doing so, soluble hK5His also promotes long-term survival, with 53% of U87-hK5His-GFP-implanted mice surviving past 120 days. We postulate that upon stereotactic implantation of our *ex vivo* retrovirally engineered hK5His glioma cells, stable integration and sustained expression of the hK5His transgene in target U87 cells provided continuous release of soluble hK5His within the loco-regional tumor microenvironment, resulting in potent suppression of tumor growth. We speculate that tumor-targeted delivery of hK5His via viral vectors such as pseudotyped retrovectors (24) and other gene delivery platforms would lead to similar results.

In summary, we provide compelling evidence that secreted hK5His protein expressed by engineered glioma cells possesses potent antiangiogenic as well as novel antimacrophage properties that block glioma progression and promote survival in an orthotopic experimental brain cancer model. Further studies on the pleiotropic effects of K5 peptide on host-derived angiogenic and macrophage response may offer new avenues of exploration for the development of therapeutic strategies for the treatment of glioma and other loco-regional refractory malignancies such as prostate and ovarian cancer.

Acknowledgments

Received 2/15/2005; revised 6/27/2005; accepted 7/7/2005.

Grant support: Canadian Prostate Cancer Research Initiative-Canadian Institutes of Health Research doctoral award (S.R. Perri), U.S. Army Medical Research and Materiel Command Breast Cancer Research predoctoral traineeship award DAMD17-03-1-0545 (S.R. Perri), Canadian Institutes of Health Research Clinician-Scientist award MOP-15017 (J. Galipeau). National Scholar of Fonds de la Recherche en Santé du Québec-Fonds pour la formation de Chercheurs et l'Aide à la Recherche (J. Nalbantoglu), Killam scholar (J. Nalbantoglu), National Cancer Institute of Canada (J. Nalbantoglu), and Valorisation-Recherche Québec (J. Nalbantoglu). B. Annabi holds a Canada Research Chair in Molecular Oncology from the CIHR.

The costs of publication of this article were defrayed in part by the payment of page charges. This article must therefore be hereby marked *advertisement* in accordance with 18 U.S.C. Section 1734 solely to indicate this fact.

References

1. Bello L, Giussani C, Carrabba G, Pluderi M, Costa F, Bikfalvi A. Angiogenesis and invasion in Gliomas. In: Kirsch M, Black PM, editors. Norwell: Kluwer; 2004. p. 263–84.
2. Holland EC. Glioblastoma multiforme: the terminator. Proc Natl Acad Sci U S A 2000;97:6242–4.
3. Black PM. Brain tumor. Part 2. N Engl J Med 1991; 324:1555–64.
4. Folkman J. Tumor angiogenesis: therapeutic implications. N Engl J Med 1971;285:1182–6.
5. Maher EA, Furnari FB, Bachoo RM, et al. Malignant glioma: genetics and biology of a grave matter. Genes Dev 2001;15:1311–33.
6. Puduvalli VK. Inhibition of angiogenesis as a therapeutic strategy against brain tumors. In: Kirsch M, Black PM, editors. Norwell: Kluwer; 2004. p. 307–36.
7. Bello L, Carrabba G, Giussani C, et al. Low-dose chemotherapy combined with an antiangiogenic drug reduces human glioma growth *in vivo*. Cancer Res 2001;61:7501–6.
8. Bello L, Giussani C, Carrabba G, et al. Suppression of malignant glioma recurrence in a newly developed animal model by endogenous inhibitors. Clin Cancer Res 2002;8:3539–48.
9. Gorski DH, Beckett MA, Jaskowiak NT, et al. Blockage of the vascular endothelial growth factor stress response increases the antitumor effects of ionizing radiation. Cancer Res 1999;59:3374–8.
10. Griscelli F, Li H, Cheong C, et al. Combined effects of radiotherapy and angiostatin gene therapy in glioma tumor model. Proc Natl Acad Sci U S A 2000;97: 6698–703.
11. Hwu WJ, Raizer J, Panageas KS, Lis E. Treatment of metastatic melanoma in the brain with temozolomide and thalidomide. Lancet Oncol 2001;2:634–5.
12. Li L, Rojiani A, Siemann DW. Targeting the tumor vasculature with combretastatin A-4 disodium phosphate: effects on radiation therapy. Int J Radiat Oncol Biol Phys 1998;42:899–903.
13. Mauceri HJ, Hanna NN, Beckett MA, et al. Combined effects of angiostatin and ionizing radiation in antitumour therapy. Nature 1998;394:287–91.
14. O'Reilly MS, Holmgren L, Chen C, Folkman J. Angiostatin induces and sustains dormancy of human primary tumors in mice. Nat Med 1996;2:689–92.
15. O'Reilly MS, Boehm T, Shing Y, et al. Endostatin: an endogenous inhibitor of angiogenesis and tumor growth. Cell 1997;88:277–85.
16. Shir A, Levitzki A. Gene therapy for glioblastoma: future perspective for delivery systems and molecular targets. Cell Mol Neurobiol 2001;21:645–56.
17. Kirsch M, Strasser J, Allende R, Bello L, Zhang J, Black PM. Angiostatin suppresses malignant glioma growth *in vivo*. Cancer Res 1998;58:4654–9.
18. O'Reilly MS, Holmgren L, Shing Y, et al. Angiostatin: a novel angiogenesis inhibitor that mediates the suppression of metastases by a Lewis lung carcinoma. Cell 1994;79:315–28.
19. Cao Y, Chen A, An SS, Ji RW, Davidson D, Llinas M. Kringle 5 of plasminogen is a novel inhibitor of endothelial cell growth. J Biol Chem 1997;272:22924–8.
20. Cao Y, Ji RW, Davidson D, et al. Kringle domains of human angiostatin. Characterization of the antiproliferative activity on endothelial cells. J Biol Chem 1996;271:29461–7.
21. Cao R, Wu HL, Veitonmaki N, et al. Suppression of angiogenesis and tumor growth by the inhibitor K1-5 generated by plasmin-mediated proteolysis. Proc Natl Acad Sci U S A 1999;96:5728–33.
22. Ory DS, Neugeboren BA, Mulligan RC. A stable human-derived packaging cell line for production of high titer retrovirus/vesicular stomatitis virus G pseudotypes. Proc Natl Acad Sci U S A 1996;93:11400–6.
23. Ponten J, Macintyre EH. Long term culture of normal and neoplastic human glia. Acta Pathol Microbiol Scand 1968;74:465–86.
24. Galipeau J, Li H, Paquin A, Sicilia F, Karpati G, Nalbantoglu J. Vesicular stomatitis virus G pseudotyped retrovector mediates effective *in vivo* suicide gene delivery in experimental brain cancer. Cancer Res 1999;59:2384–94.
25. Eliopoulos N, Galipeau J. Green fluorescent protein. In: Hicks BW, editor. Totowa: Humana Press Inc.; 2002. p. 353–71.
26. Annabi B, Lachambre MP, Bousquet-Gagnon N, Page M, Gingras D, Beliveau R. Green tea polyphenol (-)-epigallocatechin 3-gallate inhibits MMP-2 secretion and MT1-MMP-driven migration in glioblastoma cells. Biochim Biophys Acta 2002;1542:209–20.
27. Stagg J, Lejeune L, Paquin A, Galipeau J. Marrow stromal cells for interleukin-2 delivery in cancer immunotherapy. Hum Gene Ther 2004;15:597–608.
28. Li H, onso-Vanegas M, Colicos MA, et al. Intracerebral adenovirus-mediated p53 tumor suppressor gene therapy for experimental human glioma. Clin Cancer Res 1999;5:637–42.
29. Chang Y, Mochalkin I, McCance SG, Cheng B, Tulinsky A, Castellino FJ. Structure and ligand binding determinants of the recombinant kringle 5 domain of human plasminogen. Biochemistry 1998;37:3258–71.
30. Ji WR, Barrientos LG, Llinas M, et al. Selective inhibition by kringle 5 of human plasminogen on endothelial cell migration, an important process in angiogenesis. Biochem Biophys Res Commun 1998;247: 414–9.
31. Leek RD, Lewis CE, Whitehouse R, Greenall M, Clarke J, Harris AL. Association of macrophage infiltration with angiogenesis and prognosis in invasive breast carcinoma. Cancer Res 1996;56:4625–9.
32. Richter G, Kruger-Krasagakes S, Hein G, et al. Interleukin 10 transfected into Chinese hamster ovary cells prevents tumor growth and macrophage infiltration. Cancer Res 1993;53:4134–7.
33. Sunderkotter C, Steinbrink K, Goebeler M, Bhardwaj R, Sorg C. Macrophages and angiogenesis. J Leukoc Biol 1994;55:410–22.
34. Nishie A, Ono M, Shono T, et al. Macrophage infiltration and heme oxygenase-1 expression correlate with angiogenesis in human gliomas. Clin Cancer Res 1999;5:1107–13.
35. Gonzalez-Gronow M, Kalfa T, Johnson CE, Gawdi G, Pizzo SV. The voltage-dependent anion channel is a receptor for plasminogen kringle 5 on human endothelial cells. J Biol Chem 2003;278:27312–8.
36. Moser TL, Stack MS, Asplin I, et al. Angiostatin binds ATP synthase on the surface of human endothelial cells. Proc Natl Acad Sci U S A 1999;96:2811–6.
37. Troyanovsky B, Levchenko T, Mansson G, Matvijenko O, Holmgren L. Angiomotin: an angiostatin binding protein that regulates endothelial cell migration and tube formation. J Cell Biol 2001;152:1247–54.
38. Tarui T, Miles LA, Takada Y. Specific interaction of angiostatin with integrin $\alpha(v)\beta(3)$ in endothelial cells. J Biol Chem 2001;276:39562–8.
39. Moulton KS, Vakili K, Zurakowski D, et al. Inhibition of plaque neovascularization reduces macrophage accumulation and progression of advanced atherosclerosis. Proc Natl Acad Sci U S A 2003;100: 4736–41.